Multilayered Core–Shell Structure of the Dispersed Phase in High-Impact Polypropylene

Yong Chen,[1] Ye Chen,[1] Wei Chen,[2] Decai Yang[1]

[1]*State Key Laboratory of Polymer Physics and Chemistry, Changchun Institute of Applied Chemistry, Graduate School of the Chinese Academy of Sciences, Chinese Academy of Sciences, Changchun 130022, People's Republic of China*
[2]*Beijing Research Institute of Chemical Industry, China Petroleum & Chemical Corporation, Beijing 100013, People's Republic of China*

Received 18 January 2005; accepted 9 November 2005
DOI 10.1002/app.25410
Published online 19 February 2008 in Wiley InterScience (www.interscience.wiley.com).

ABSTRACT: The multiphase morphology of high impact polypropylene (hiPP), which is a reactor blend of polypropylene (PP) with ethylene–propylene copolymer, was investigated by transmission electron microscopy, selected area electron diffraction, atomic force microscopy, and field-emission scanning electron microscopy techniques in conjunction with an analysis of the hiPP composition and chain structure based on solvent fractionation, ^{13}C-NMR, and differential scanning calorimetry measurements. A multilayered core–shell structure of the dispersed phase of hiPP in solution-cast films and the bulk was observed. The inner core was mainly composed of polyethylene (including its long blocks) together with part of PP, the intermediate layer was ethylene–propylene random copolymer, and the outer shell consisted of ethylene–propylene multiblock copolymers. The formation process and controlling factors of the multilayered core–shell structure are discussed. This kind of multiphase morphology of hiPP caused the material to possess both a high rigidity and high toughness. © 2008 Wiley Periodicals, Inc. J Appl Polym Sci 108: 2379–2385, 2008

Key words: core–shell polymers; crystallization; morphology; phase behavior; poly(propylene) (PP)

INTRODUCTION

High-impact polypropylene (hiPP) produced by a multistage polymerization process is a kind of reactor blend of polypropylene (PP) with ethylene–propylene copolymers.[1–3] The blend has a uniform distribution of rubbery phase in PP matrix and exhibits a high rigidity and toughness. hiPP is a complex multicomponent blending system, consisting of the PP matrix, ethylene–propylene random copolymer (EPR), ethylene–propylene multiblock copolymer (PE-*b*-PP), and a small amount of polyethylene (PE).[4–8] The interchain continuity and intrachain polydispersity are two characteristics of hiPP chain composition.

The performances of hiPP are closely related to the multiphase structure of this material.[2,3,9–12] The formation of the finely dispersed phase in hiPP is determined by the composition, chain structure, interfacial interaction between phases, viscosity ratio of dispersed phase to matrix, polymerization, and processing parameters. A core–shell structure of the dispersed phase, which is generally considered to be PE inclusions encapsulated by a ethylene–propylene rubber shell, is usually observed in hiPP.[13–16] This core–shell structure has proven to be efficient for the toughness–rigidity balance of hiPP.

Although the production of hiPP is a commercial success, the understanding of its material structure is far from perfect. Generally, with cryoultramicrotomy, staining, and surface etching techniques, one can obtain some information about the hiPP bulk-phase structure.[2,3,5,9–16] However, it is difficult to obtain the structural details of this material. In this study, the morphologies of hiPP in solution-cast thin films and the bulk were investigated, and a multilayered core–shell structure of the dispersed phase in hiPP was revealed, which should be helpful in the understanding of the structure–property relations of this material.

EXPERIMENTAL

Materials and sample preparation

The hiPP sample used in this work was a commercial product in pellet form, synthesized in a multistage polymerization process. The tensile modulus of the material was 1030 MPa, and the notched charpy impact strength at 23 and −20°C were 15.5 and 8.1 kJ/m^2, respectively. The weight-average molecular weight and polydispersity index (weight-average molecular weight/number-average molecular weight) of hiPP were 160,000 and 4.1, respectively, as measured by gel

Correspondence to: D. Yang (dcyang@ciac.jl.cn).
Contract grant sponsor: National Basic Research Program of China; contract grant number: 2005CB623800.
Contract grant sponsor: Chinese Academy of Sciences; contract grant number: KJCX2-SW-H07.

Journal of Applied Polymer Science, Vol. 108, 2379–2385 (2008)

TABLE I
Composition and Chain Sequence Distribution of hiPP and the Fractions Based on ^{13}C-NMR

	Molar composition (%)		Molar composition of the Triads (%)					
Sample	P	E	PPP	PPE	EPE	EEE	EEP	PEP
hiPP	72.7	27.3	51.8	15.4	5.5	8.3	11.8	7.0
f_a	63.0	37.0	27.5	16.1	18.7	5.5	10.3	21.9
f_b	64.5	35.5	53.4	7.1	4.0	24.0	8.7	2.9
f_c	97.5	2.5	97.0	0.6	0.1	2.0	0.3	0.1

permeation chromatography. Three fractions of hiPP were also obtained by successive solvent extraction. hiPP was dissolved in xylene at 130°C, and then, the solution was gradually cooled to room temperature. The precipitate was separated from the solution by filtration. Solvent in the remaining clear solution was evaporated, and some rubbery component was obtained as fraction f_a. The filtered precipitate was extracted by xylene at 100°C, and two fractions were obtained after solvent evaporation: the dissolved part as fraction f_b and the remainder as fraction f_c. The composition and chain structure of hiPP and its three fractions were measured by ^{13}C-NMR.

Thin films of hiPP were prepared by the casting of a 0.1 wt % xylene solution onto a carbon-coated mica surface at 130°C. After solvent evaporation, the specimens were cooled to room temperature at 1°C/min and then vacuum-dried at room temperature for 24 h. Thin sections of the bulk samples were prepared by cryoultramicrotomy of the hiPP pellets with a Leica Ultracut R microtome (Vienna, Austria) operated at −80°C and at a cutting speed of 1 mm/s. Bulk samples were also fractured in liquid nitrogen and then etched in xylene at room temperature for 30 min.

Atomic force microscopy (AFM)

The solution-cast thin films supported by mica were studied by AFM. Height and phase images were obtained simultaneously by a SPA-HV300 with a SPI 3800N controller (Seiko Instruments Industry Co., Ltd., Tokyo, Japan) operated in tapping mode at ambient conditions. A 150-μm scanner was selected. A silicon cantilever with a resonant frequency of 70–80 kHz and a spring constant of 2 N/m was used.

Transmission electron microscopy (TEM)

For TEM observations, the thin films were transferred onto the surface of water and collected on copper grids. A Jeol 1011 transmission electron microscope (Tokyo, Japan) operated at 100 kV was used. Bright-field (BF) electron micrographs were obtained by defocusing of the objective lens.[17] The camera length of the electron diffraction measurement was calibrated with Au.

Field-emission scanning electron microscopy

The cryofractured surface of bulk hiPP after solvent extraction was coated with Au and then examined with an XL30 ESEM field-emission gun (FEG) scanning electron microscope (FEI Co., Hillsboro, OR) at an accelerating voltage of 20 kV.

Differential scanning calorimetry (DSC)

DSC measurements were carried out with a Perkin Elmer diamond differential scanning calorimeter (Shelton, CT) under a protective nitrogen atmosphere at cooling and reheating rates of 10°C/min.

RESULTS AND DISCUSSION

Composition and chain structure of hiPP and the fractions

The composition and chain sequence distribution of hiPP and the fractions are shown in Table I on the basis of ^{13}C-NMR measurement. The ethylene content of the hiPP was fairly high (27.3 mol %), and the compositions of the ethylene–propylene copolymers in hiPP were quite complicated. However, from ^{13}C-NMR data of the three fractions, a general understanding about the hiPP chain structure was obtained. Here fraction f_a, which was soluble in xylene at room temperature, was mainly composed of EPRs (amorphous EPRs; see also the DSC results given later), but short PE and PP segments were also present. In addition, the existence of a small amount of low-molecular-weight PP and PE could not be ruled out. Fraction f_b, which was the soluble fraction in xylene at 100°C, should consist of a broad range of segmented ethylene–propylene copolymers with different block lengths (see also the DSC and TEM results given later), and some PE homopolymers may have also been included, whereas fraction f_c (the insoluble fraction in xylene at 100°C) was mainly composed of PP homopolymers.[4–8] Apparently, there was a continuous distribution of interchain composition and an intrachain heterogeneity of hiPP chain structure. The weight fractions of f_a, f_b, and f_c in hiPP were 21.6, 11.4, and 67.0%, respectively, which suggests that in hiPP, the PP homopolymers (f_c) constituted the matrix and

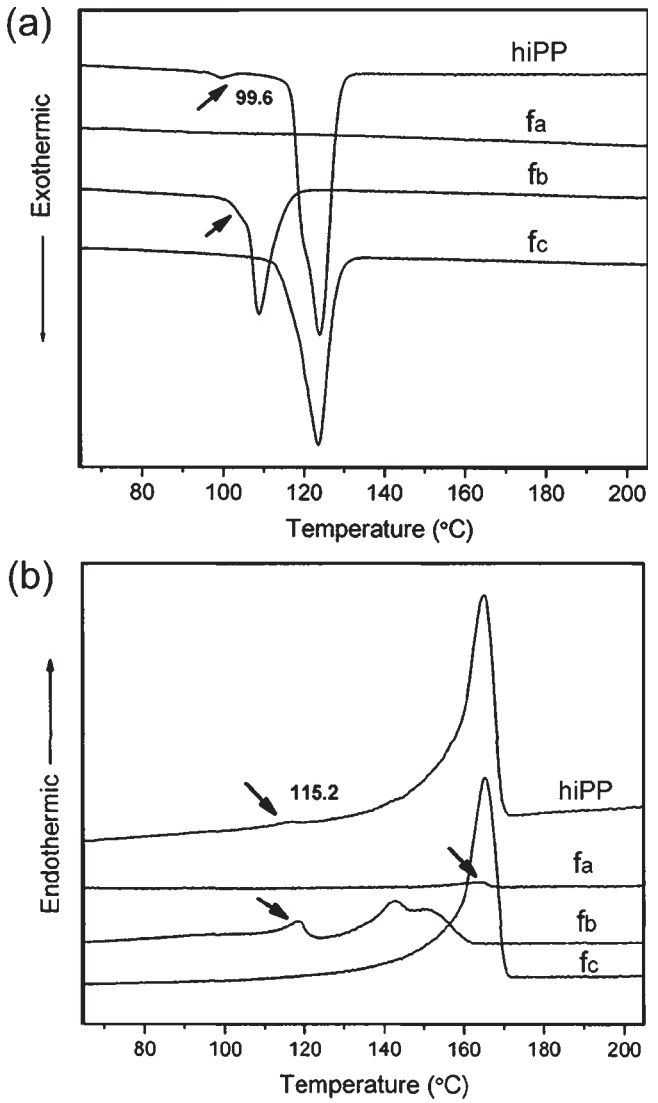

Figure 1 DSC (a) cooling and (b) reheating curves of hiPP and the fractions at a scanning rate of 10°C/min after melting at 210°C for 5 min.

provided enough rigidity, whereas the rubbery component (f_a) played a role as a toughening agent with the aid of segmented ethylene–propylene copolymers (f_b).

Thermal behavior of hiPP and the fractions

The crystallization and melting behavior of hiPP and the fractions are shown in Figure 1. For hiPP (unfractionated), in the DSC cooling and reheating curves, in addition to the crystallization (123.0°C) and melting (164.0°C) peaks of PP, there existed a weak crystallization peak (99.6°C) and a weak melting peak (115.2°C), which were attributed to the crystallization and melting of PE crystals, respectively. For fraction f_a, there was no crystallization peak, but a weak melting peak was still observed at about 164.0°C, which indicated the presence of a small amount of PP crystallites. As for fraction f_b, in the cooling curve, there existed a main crystallization peak and a shoulder peak at a lower temperature, which should have corresponded, respectively, to crystallizations of PP and PE (including the blocks and some homopolymers), whereas in the reheating curve, three melting peaks were observed, in which the one at lower temperature corresponded to PE crystal melting and the two at high temperatures corresponded to PP crystals formed by PP blocks with different lengths.[7,8] For fraction f_c, the DSC cooling and reheating curves showed typical thermal behavior of the PP homopolymer. The DSC results were consistent with that of the ^{13}C-NMR analysis.

Phase morphology of hiPP solution-cast thin films

The BF electron micrograph of the hiPP solution-cast thin film at 130°C displayed a multiphase morphology (Fig. 2). Well-defined core–shell particles, with diameter of about 0.5–2.0 μm, dispersed uniformly in a PP matrix. The matrix of the film mainly consisted of lathlike lamellae of PP with the *c* axis perpendicular to film plane,[18] whereas the dispersed particles clearly demonstrated a multilayered core–shell morphology with the inner core, intermediate layer, and outer shell (the dark ring), as indicated in the magnified image of a particle (Fig. 2 inset).

To identify the material composition of different phases in the multilayered core–shell structure, selected area electron diffraction (SAED) observations

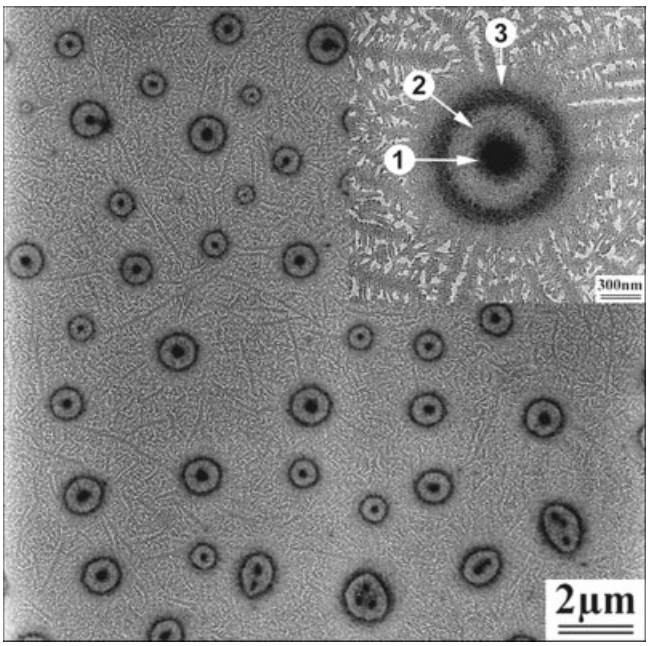

Figure 2 BF electron micrograph of hiPP solution-cast thin-film at 130°C showing the multilayered core–shell particles dispersed in the PP matrix. The inset shows magnified image of a particle with the (1) inner core, (2) intermediate layer, and (3) outer shell, as indicated.

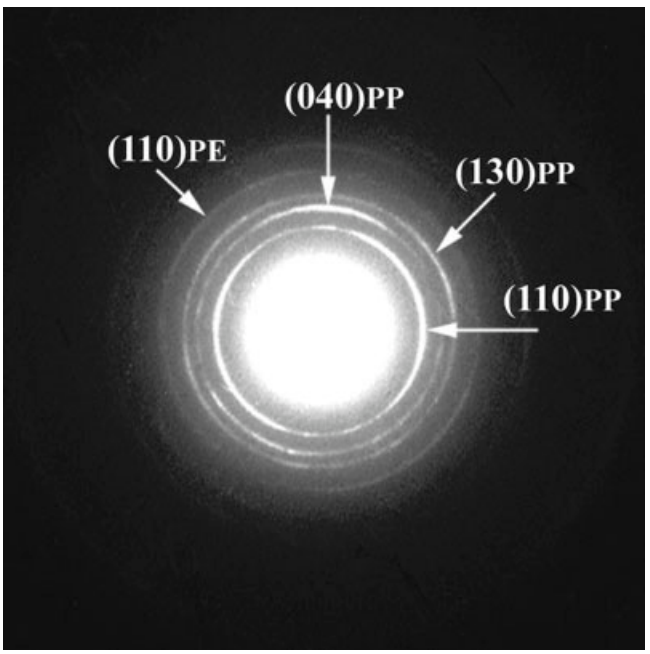

Figure 3 SAED pattern corresponding to the core area of the multilayered core–shell particle.

were carried out. Figure 3 shows a SAED pattern of the core area. A (110) diffraction ring of PE crystals was observed, indicating the existence of ethylene homopolymer and its long blocks in the core regions. In fact, the PE lamellae in the core regions were directly observed in the TEM BF image if the film was thin enough. As shown in Figure 4, the random distributed dark lines in the core region represent PE lamellae with an average thickness of about 20 nm. In addition to the (110) reflection of PE, there existed (110), (040), and (130) reflections (rings or arcs) of PP crystals in the core regions (Fig. 3). This implies that during the film formation and phase separation processes, PP (including part of its blocks) could not be completely rejected from the core regions of PE. The PP may have been included in the PE phases or located at the bottom surface of the core regions. For the intermediate layer of the multilayered core–shell morphology, which corresponded to the shell of the PE/EPR core–shell structure reported in hiPP or PP/EPR/PE ternary blends;[13–16,19–21] we believe that it was mainly composed of amorphous EPR, according to the weak contrast of this layer in the TEM BF image (Figs. 2 and 4) and the AFM results shown later. What was more interesting here was the composition of the outer shell (the dark ring) in the multilayered core–shell structure. Surprisingly, the SAED pattern (Fig. 5) of this layer exhibited a set of six symmetric reflection spots besides the (110), (040), and (130) reflection rings of PP. The *d* spacing corresponding to the six reflection spots was 4.22 ± 0.02 Å, which coincided well with the *d* value (4.23 Å) of the hexagonal form crystals of PE.[22] The symmetric six reflection spots were attributed to (100) reflection of hexagonal PE, which was recently found in segmented ethylene–propylene copolymers.[23–26] The explanation proposed in the literature for the presence of the PE hexagonal phase at atmospheric pressure was that defects in the form of side groups stabilized the PE hexagonal phase at ambient conditions. The results observed in this study should also correspond with this, as there was a broad distribution of chain

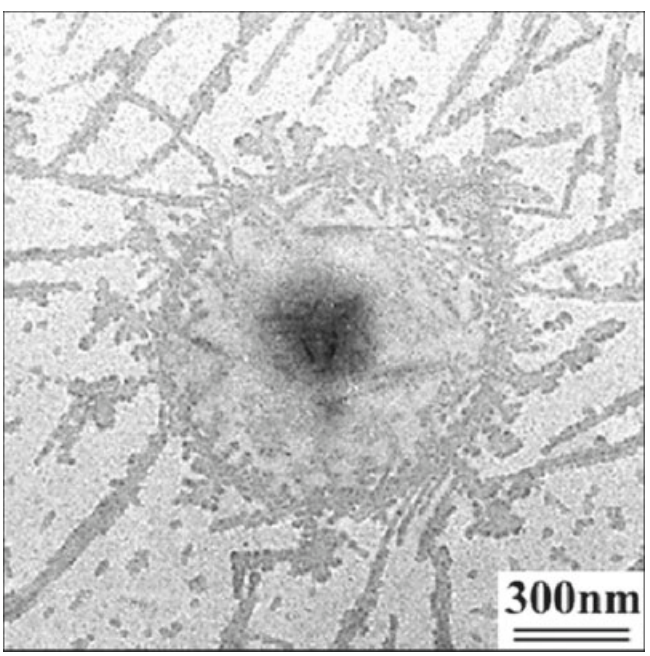

Figure 4 BF electron micrograph of a particle in an ultrathin solution-cast film of hiPP. The randomly distributed dark lines in the core area represent PE lamellae.

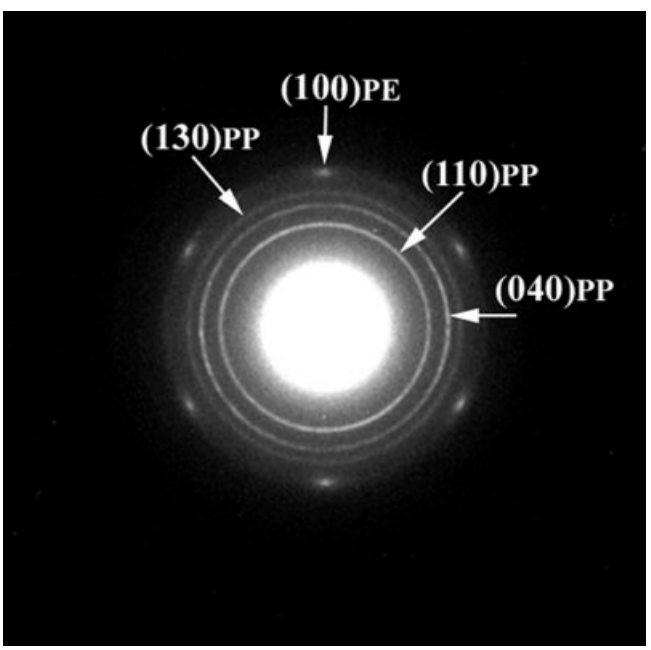

Figure 5 SAED pattern corresponding to the outer shell (the dark ring) of the multilayered core–shell particle.

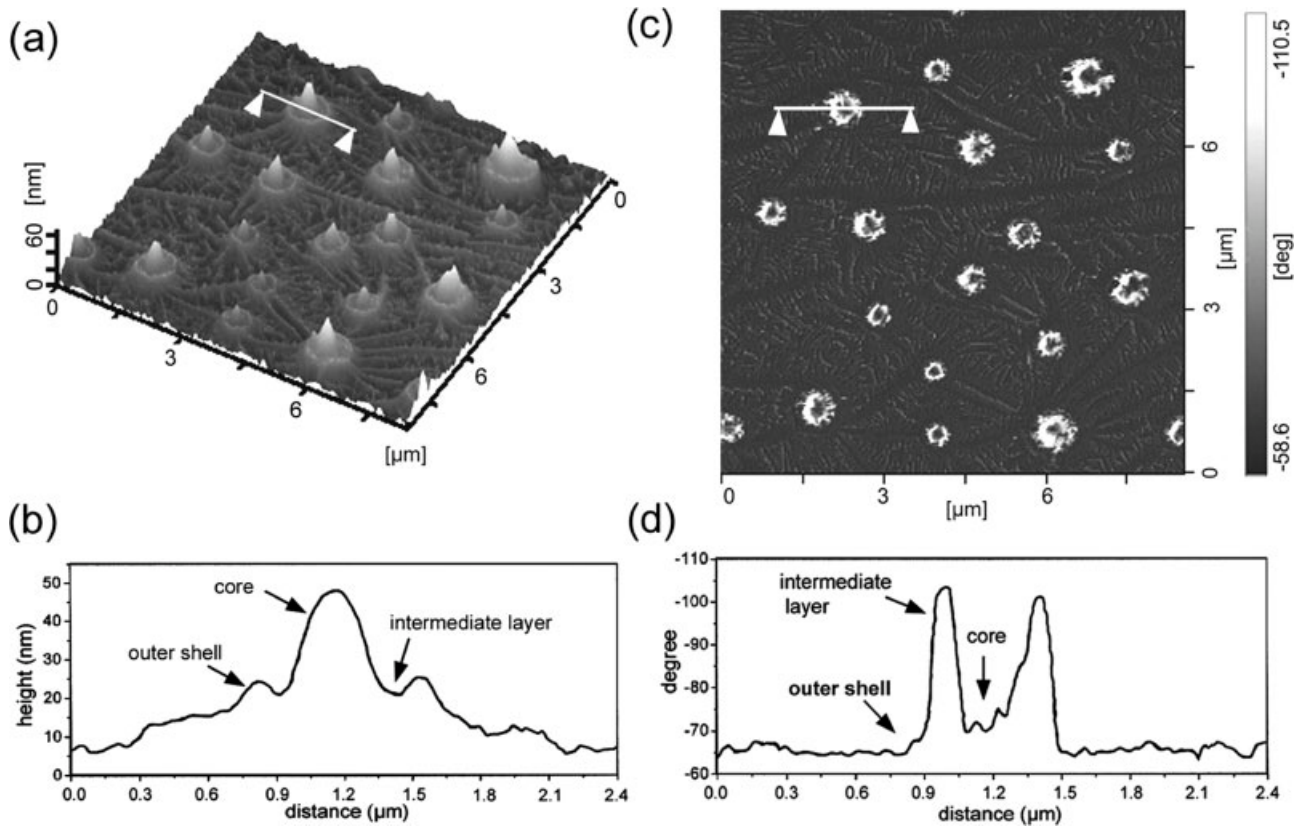

Figure 6 AFM (a) height image and (c) corresponding phase image of the solution-cast thin film of hiPP together with the (b and d) cross-sectional views of a particle along the lines as indicated by the arrows in the height and phase images, respectively.

composition of the ethylene–propylene segmented copolymers presented in hiPP. These results indicate that the outer shell of the multilayered core–shell morphology of hiPP consisted of PE and PP crystallites formed by the (PE-*b*-PP)s with short blocks.

The surface topographic features of hiPP solution-cast thin films were examined with AFM. Figure 6 shows the AFM height image and corresponding phase contrast image of the film together with the cross-sectional views of a particle along the lines indicated by the arrows in the height and phase images, respectively. It is known that the brightness contrast in AFM height image represents the height difference, whereas that in the phase image generally reflects the soft and hard natures of the sample.[27,28] The AFM height image [Fig. 6(a,b)] showed that the dispersed particles protruded from the film plane with an average height of about 50 nm, which implied a serious aggregation of phase-separated components in the PP matrix. The dispersed particles were not spherical. Each of them had a main peak and a shoulder rim around the peak [as indicated in Fig. 6(b)], which corresponded to the inner core and the outer shell as observed by TEM (Fig. 2), whereas the valley between the main peak and shoulder rim should have been the intermediate EPR layer, which was confirmed by the phase image. Figure 6(c,d) shows the corresponding phase images. Clearly, the strong contrast (phase lag) between the intermediate layer and the matrix implied a soft nature of the intermediate layer (EPR), whereas the weak contrast between the core and the matrix implied that the hardness of the core (PE inclusions) was slightly lower than that of the

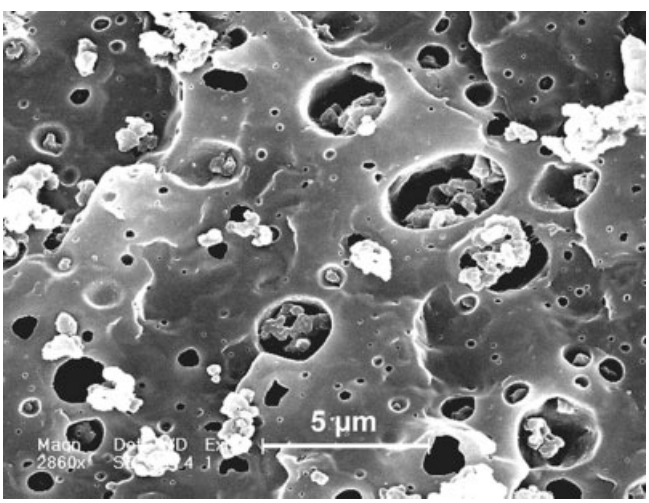

Figure 7 Field-emission scanning electron microscopy micrograph of the cryofractured surface of bulk hiPP after extraction with xylene.

matrix (PP). The phase contrast of the outer shell seemed to be the same as the PP matrix, which was due to the coexistence of PE and PP crystallites in this layer, as revealed by TEM observation.

Multiphase morphology of hiPP in the bulk

The performance of hiPP is directly related to its bulk-phase morphologies. The multiphase morphology of the bulk samples of hiPP could clearly be seen from the cryofractured surface of hiPP after the EPR was removed by solvent. As shown in Figure 7, the dispersed rubbery phase, about 1.0–3.0 μm in diameter, displayed a typical core–shell structure in the PP matrix. This result seems consistent with most of the reports on the phase morphology of bulk hiPP after melt processing; that is, the PE inclusion was surrounded by a single EPR shell. However, in the BF electron micrograph (Fig. 8) of the ultrasectioned thin film of the bulk hiPP (pellets), a multilayered core–shell structure of the dispersed phase was revealed, in which the darker core and outer shell arose from the higher contrast of PE crystals enriched in these regions compared with that of PP matrix, which implied a similar structure to that formed in the solution-cast films.

These observations indicate the dispersed particles in hiPP consisted of a relatively hard PE core and outer shell and an intermediate soft rubbery layer. In addition, there should have been a transitional layer between the PP matrix and the particle, which provided effective bonding strength.[16,20] This special kind of core–shell impact modifier is considered to be important for an optimum balance between toughness and stiffness in hiPP because it can efficiently deform through fibrillized cavitation processes, which initiates the multiple crazing or shear flow of the matrix material.[29–32]

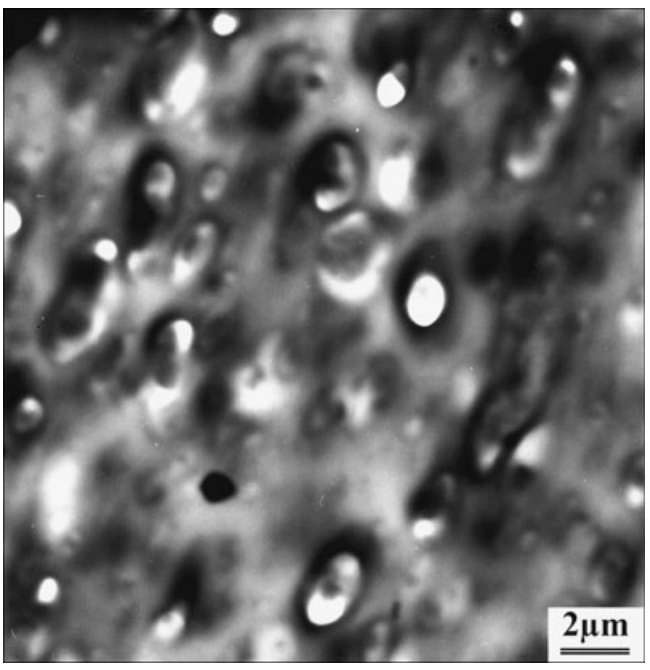

Figure 8 BF electron micrograph of hiPP thin film ultramicrotomed from the bulk sample (the pellets).

Unambiguously, the formation of the multiphase morphology of hiPP in the solution-cast thin film and the bulk resulted from the complexity of the composition and immiscibility between the various components of hiPP. For the solution-cast film, during the solvent evaporation and film-formation processes, the phase separations of PE (including its long blocks) and EPR took place first, which resulted in PE/EPR core–shell structure formation. This was similar to PP/EPR/PE ternary blends, in which a core–shell morphology of PE core encapsulated by EPR shell is usually formed.[19–21] Theoretical models based on interfacial free energy and spreading coefficient can well explain this core–shell morphology formation.[21,33,34] In other words, interfacial interaction (or interfacial tension) between phases was a major factor that controlled the phase structure. The dominant morphology was that with the lowest interfacial free energy. However, the presence of (PE-*b*-PP)s made the phase structure of hiPP more complicated than that of simple PP/EPR/PE ternary blends. During subsequent crystallization process of PP, further phase separation took place, and the (PE-*b*-PP)s s were rejected from the PP matrix to the periphery of previously formed PE/EPR core–shell structure, which resulted in the outer shell of the multilayered core–shell morphology of hiPP. It is known that interfacially active ethylene–propylene block copolymers can play the role of compatibilizer to enhance interfacial adhesion between the EPR and PP phases.[7,14,16,35] Thus, the outer shell of multilayered core–shell structure can be considered a compatibilizing layer bridging the EPR phase (intermediate layer) with the PP matrix. The similar phase morphology formed in bulk hiPP implied that this multistage phase separation process between the different components of hiPP occurred in the melt processing process,[36] which determined the multiphase morphology and the mechanical properties of the toughness–rigidity balance of the material.

CONCLUSIONS

hiPP is a complex multicomponent and multiphase blend. The dispersed phase in hiPP exhibited a multilayered core–shell structure, in which the inner core, intermediate layer, and outer shell were mainly composed of PE (including PE long blocks), EPR, and PE–PP multiblock copolymers, respectively. It was the (PE-*b*-PP)s in hiPP that formed the outer shell of the multilayered core–shell morphology, which could be considered a compatibilizing layer bridging the inter-

mediate layer (EPR phase) and the PP matrix. It was the multilayered core–shell morphology that made the material possess both high rigidity and high toughness.

References

1. Galli, P.; Haylock, J. C. Prog Polym Sci 1991, 16, 443.
2. Debling, J. A.; Ray, W. H. J Appl Polym Sci 2001, 81, 3085.
3. Kittilsen, P.; Mckenna, T. F. J Appl Polym Sci 2001, 82, 1047.
4. Mirabella, F. M., Jr. Polymer 1993, 34, 1729.
5. Usami, T.; Gotoh, Y.; Umemoto, H.; Takayama, S. J Appl Polym Sci Appl Polym Symp 1993, 52, 145.
6. Cai, H.; Luo, X.; Ma, D.; Wang, J.; Tan, H. J Appl Polym Sci 1999, 71, 93.
7. Fan, Z.; Zhang, Y.; Xu, J.; Wang, H.; Feng, L. Polymer 2001, 42, 5559.
8. Xu, J.; Feng, L.; Yang, S.; Wu, Y.; Yang, Y.; Kong, X. Polymer 1997, 38, 4381.
9. Urdampilleta, I.; González, A.; Iruin, J. J.; de la Cal, J. C.; Asua, J. M. Macromolecules 2005, 38, 2795.
10. Cecchin, G.; Marchetti, E.; Baruzzi, G. Macromol Chem Phys 2001, 202, 1987.
11. McKenna, T. F.; Bouzid, D.; Matsunami, S.; Sugano, T. Polym React Eng 2003, 11, 177.
12. Cai, H.; Luo, X.; Chen, X.; Ma, D.; Wang, J.; Tan, H. J Appl Polym Sci 1999, 71, 103.
13. Radusch, H.; Doshev, P.; Lohse, G. Polimery 2005, 50, 279.
14. Tan, H.; Li, L.; Chen, Z.; Song, Y.; Zheng, Q. Polymer 2005, 46, 3522.
15. Pegoraro, M.; Severini, F.; Di Landro, L.; Braglia, R.; Kolarik, J. Macromol Mater Eng 2000, 280/281, 14.
16. Ito, J.; Mitani, K.; Mizutani, Y. J Appl Polym Sci 1992, 46, 1221.
17. Miles, M. J.; Petermann, J. J Macromol Sci Phys 1979, 16, 243.
18. Shen, Y.; Yang, D.; Feng, Z. J Mater Sci 1991, 26, 1941.
19. Petrović, Z. S.; Budinski-Simendić, J.; Divjaković, V.; Škrbić, Ž. J Appl Polym Sci 1996, 59, 301.
20. Ito, J.; Mitani, K.; Mizutani, Y. J Appl Polym Sci 1985, 30, 497.
21. Hemmati, M.; Nazokdast, H.; Panahi, H. S. J Appl Polym Sci 2001, 82, 1129.
22. Bassett, D. C.; Block, S.; Piermarini, G. J. J Appl Phys 1974, 45, 4146.
23. Hu, W.; Srinivas, S.; Sirota, E. B. Macromolecules 2002, 35, 5013.
24. Bracco, S.; Comotti, A.; Simonutti, R.; Camurati, I.; Sozzani, P. Macromolecules 2002, 35, 1677.
25. Wright, K. J.; Lesser, A. J. Macromolecules 2001, 34, 3626.
26. Lieser, G.; Wegner, G.; Smith, J. A.; Wagener, K. B. Colloid Polym Sci 2004, 282, 773.
27. Tanem, B. S.; Kamfjord, T.; Augestad, M.; Løvgren, T. B.; Lundquist, M. Polymer 2003, 44, 4283.
28. Wang, H.; Djurišić, A. B.; Chan, W. K.; Xie, M. H. Appl Surf Sci 2005, 252, 1092.
29. Cruz-Ramos, C. A. In Polymer Blends. Volume 2: Performance; Paul, D. R.; Bucknall, C. B., Eds.; Wiley: New York, 2000; Chapter 24.
30. Kim, G. M.; Michler, G. H.; Gahleitner, M.; Fiebig, J. J Appl Polym Sci 1996, 60, 1391.
31. Kim, G. M.; Michler, G. H.; Gahleitner, M.; Mülhaupt, R. Polym Adv Technol 1998, 9, 709.
32. Starke, J. U.; Godehardt, R.; Michler, G. H.; Bucknall, C. B. J Mater Sci 1997, 32, 1855.
33. Guo, H. F.; Packirisamy, S.; Gvozdic, N. V.; Meier, D. J. Polymer 1997, 38, 785.
34. Hobbs, S. Y.; Dekkers, M. E.; Watkins, V. H. Polymer 1988, 29, 1598.
35. Hudson, S. D.; Jamieson, A. M. In Polymer Blends. Volume 1: Formulation; Paul, D. R.; Bucknall, C. B., Eds.; Wiley: New York, 2000; Chapter 15.
36. Mirabella, F. M., Jr. J Polym Sci Part B: Polym Phys 1994, 32, 1205.